

Axial force imparted by a conical radiofrequency magneto-plasma thruster

C. Charles, K. Takahashi, and R. W. Boswell

Citation: *Appl. Phys. Lett.* **100**, 113504 (2012); doi: 10.1063/1.3694281

View online: <http://dx.doi.org/10.1063/1.3694281>

View Table of Contents: <http://apl.aip.org/resource/1/APPLAB/v100/i11>

Published by the [American Institute of Physics](#).

Related Articles

Generating large-area uniform microwave field for plasma excitation
Phys. Plasmas **19**, 033302 (2012)

The impact of plasma-wall interaction on the gas mixing efficiency in electron cyclotron resonance ion source
Rev. Sci. Instrum. **83**, 02A348 (2012)

Optical emission spectroscopy of the Linac4 and superconducting proton Linac plasma generators
Rev. Sci. Instrum. **83**, 02A729 (2012)

H⁻ radio frequency source development at the Spallation Neutron Source
Rev. Sci. Instrum. **83**, 02A725 (2012)

Characteristic of a triple-cathode vacuum arc plasma source
Rev. Sci. Instrum. **83**, 02A513 (2012)

Additional information on *Appl. Phys. Lett.*

Journal Homepage: <http://apl.aip.org/>

Journal Information: http://apl.aip.org/about/about_the_journal

Top downloads: http://apl.aip.org/features/most_downloaded

Information for Authors: <http://apl.aip.org/authors>

ADVERTISEMENT

NEW!

iPeerReview
AIP's Newest App



**Authors...
Reviewers...
Check the status of
submitted papers remotely!**

AIP | Publishing

Axial force imparted by a conical radiofrequency magneto-plasma thruster

C. Charles,^{a)} K. Takahashi,^{b)} and R. W. Boswell

Space Plasma, Power and Propulsion Laboratory, Research School of Physics and Engineering,
The Australian National University, ACT 0200, Australia

(Received 28 October 2011; accepted 28 February 2012; published online 13 March 2012)

Direct thrust measurements of a low pressure (~ 0.133 Pa) conical radiofrequency (rf) at 13.56 MHz argon plasma source show a total axial force of about 5 mN for an effective rf power of 650 W and a maximum magnetic field of 0.018 T, of which a measured value of 2.5 mN is imparted by the magnetic nozzle. A simplified model of thrust including contributions from the electron pressure and from the magnetic field pressure is developed. The magnetic nozzle is modelled as a “physical” nozzle of increasing cross-sectional area. © 2012 American Institute of Physics. [<http://dx.doi.org/10.1063/1.3694281>]

Charged particles’ acceleration and confinement are processes inherent to most non-magnetised and magnetised plasmas. Studies range from basic sheath treatment at a physical plasma-wall boundary¹ to plasma detachment from a magnetic nozzle.² Recent theoretical and simulation studies of the axial force imparted by a magnetised plasma have highlighted the complex role of the plasma dynamics^{3–6} (charged particles velocity distributions, collisional processes...) and its relevance to the field of space plasma physics and electric propulsion. Lately, this axial force has been directly measured in rf plasmas, confirming the role of the maximum electron pressure in the plasma source cavity^{7–9} and identifying an additional axial force produced by an electron diamagnetic drift in the expanding magnetic field.¹⁰ These results were obtained using a cylindrical radiofrequency helicon source or “thruster” of various length and diameter where the magnetic field (if applied) would be generated using one or two axial solenoids or arrays of permanent magnets. Plasma coupling and acceleration in a conical helicon plasma source contiguously attached to a small vacuum chamber has also been reported,¹¹ which showed the presence of a mode with a maximum magnetic field near the exit of the source of potential interest to plasma propulsion. Here, direct measurements of the axial force imparted by such a conical helicon plasma source are obtained and modeled. The contribution to the axial force of the plasma cavity shape is identified.

Experiments are carried out using a 19.5 cm-long conical helicon plasma source (with an inner radius varying from $r_{end} = 1.8$ cm to $r_{exit} = 4.5$ cm) attached to a grounded thrust balance^{7,9} and immersed in the 1 m-diameter 1.4 m-long *Irukandji* vacuum vessel,¹² which is pumped down to a base pressure of about 1.3×10^{-4} Pa (Figure 1). Argon gas is introduced at the closed end of the conical cavity using a 3 mm-diameter cylindrical ceramic gas injector inserted on axis (but not in contact with the cavity) through a 8 mm-diameter hole and here a constant gas flow of about 25 sccm is used to maintain an operating pressure of about 0.133 Pa measured by a baratron gauge.¹² $z = 0$ cm is defined at the

small closed end of the conical cavity and z_{exit} is 19.5 cm (Figure 1). The two axial solenoids, called the source solenoid and the exhaust solenoid, are centered at $z = 5$ cm and $z = 18$ cm, respectively (the edge of the solenoid former is located at $z = 21.5$ cm), and a 2.5 cm wide, 10.5 cm in diameter two loop antenna is centered at $z_{ant} = 10$ cm. The antenna is fed by rf power via a matching network located outside vacuum and hosting a current probe and is not in contact with either the plasma cavity or solenoids.¹⁰ Here, the measured vacuum resistance is about 0.58Ω and the measured power transfer efficiency $\frac{P_{rf\ effective}}{P_{rf\ generator}}$ is in the 80%–90% range. For zero current in the source solenoid and a current of 6 A in the exhaust solenoid, a maximum magnetic field of about 0.018 T is generated and the axial profile is shown in Figure 2 (solid line). The vacuum vessel is equipped with a movable 4 mm diameter disc Langmuir probe used to measure the axial and radial plasma parameters profile and a typical axial density profile obtained for 530 W effective rf power is shown in Figure 2 (open squares). The same data analysis method as in Ref. 7 is used with the assumption of a Maxwellian distribution for the electrons.

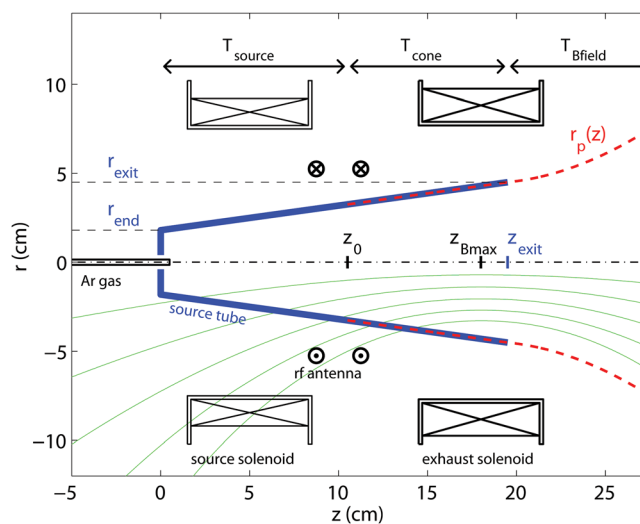


FIG. 1. (Color online) Schematic of the conical magneto-plasma thruster (the thruster is attached to a thrust balance immersed in the *Irukandji* vacuum vessel equipped with the Langmuir probe and not shown here for clarity but previously described in Refs. 7 and 12). The magnetic field lines generated by zero current in the source solenoid and 6 A in the exhaust solenoid are shown by thin solid lines.

^{a)}Electronic mail: christine.charles@anu.edu.au.

^{b)}Permanent address: Department of Electrical Engineering and Computer Science, Iwate University, Morioka 020-8551, Japan.

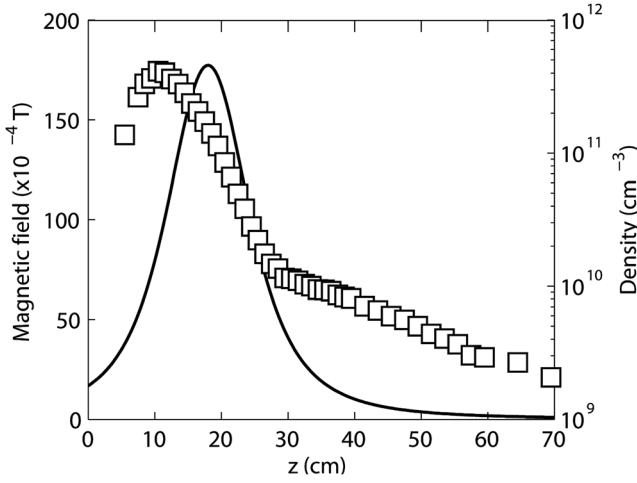


FIG. 2. Axial magnetic field $B_z(0, z)$ (solid line) and axial plasma density $n(0, z)$ (open squares) measured for an effective rf power of 530 W. The axial position of the respective maxima is $z_{Bmax} = 18$ cm and $z_0 = 10.5$ cm.

The axial force is measured as a function of the effective rf power using a previously described thrust balance (a pendulum) equipped with a laser displacement sensor.^{7,8} Two distinct experimental configurations are used:¹⁰ in the first configuration, both the solenoids and conical cavity are rigidly attached to the thrust balance to obtain the total generated axial force T_{total} ; in the second configuration, the conical cavity is independently supported by stands mounted on the vacuum vessel, and only the solenoids are rigidly attached to the thrust balance to obtain the axial force T_{Bfield} from the magnetic nozzle. The plasma generated inside the cavity and expanding in the vacuum vessel is unchanged for those two thrust balance configurations.

Figure 3 shows the maximum plasma density $n(0, z_0)$ (open squares) measured at $z_0 = 10.5$ cm on the z -axis and the measured total axial force T_{total} (open triangles) versus effective rf power: a somewhat direct correlation between total axial force and density of 1 mN per 10^{11} cm⁻³ of

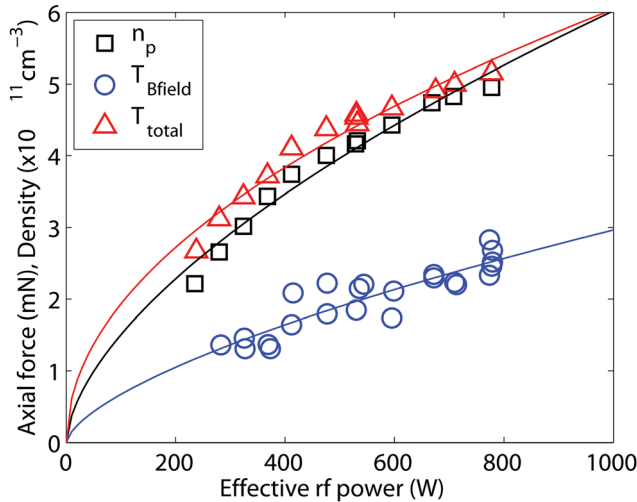


FIG. 3. (Color online) Maximum plasma density $n(0, z_0)$ measured on axis (open squares), total axial force T_{total} measured in the first thrust balance configuration (open triangles) and axial force T_{Bfield} from the magnetic nozzle measured in the second thrust balance configuration (open circles) versus effective rf power.

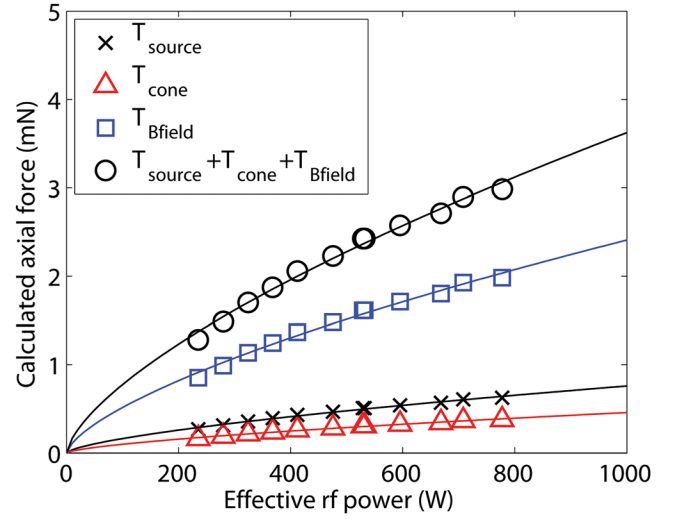


FIG. 4. (Color online) Calculated axial force T_{source} from Eq. (1) (crosses), T_{cone} from Eq. (2) (open triangles), T_{Bfield} from Eq. (3) (open squares) and the sum $T_{source} + T_{cone} + T_{Bfield}$ (open circles) versus effective rf power.

charged particles, i.e., a force of 5 mN for a density of 5×10^{11} cm⁻³ at 650 W. The axial force T_{Bfield} from the magnetic field is measured versus effective rf power in the second thrust balance configuration and the results are also plotted as open circles on Figure 3. The maximum value for T_{Bfield} is 2.5 mN at 780 W and the fraction T_{Bfield}/T_{total} is about 50% and constant with rf power. The electron temperature is quasi-constant at about 4.5 eV (± 0.25 eV), and the maximum plasma potential (at $z_0 = 10.5$ cm) increases from 39 to 47 V (± 2 V) when the effective rf power is increased from 200 to 800 W.

Although a complete description of the axial force imparted by this magneto-plasma is well beyond the scope of a letter, a simplified 1D model is developed using plasma parameters measurements. With the assumption of an isotropic electron temperature ($T_e = T_{e\perp} = T_{e\parallel}$), the electron pressure ($p_e = qn_e T_e$ with T_e in Volts) is maximum when the ion flow velocity is zero;^{7,8} assuming that the latter is verified along the single cross-sectional plane at z_0 , the axial force term T_{source} transferred to the back of the cavity (from $z = 0$ cm to $z = z_0$) is approximated similarly to a cylindrical case⁸ as

$$T_{source} = \langle p(r, z_0) \rangle_r A_0 = q \langle n_0(r, z_0) T_e(r, z_0) \rangle_r A_0, \quad (1)$$

where A_0 is the cross-sectional area at the axial position z_0 of maximum density $n(0, z_0)$ (Figure 1), $\langle p(r, z_0) \rangle_r$ is the radially averaged electron pressure measured along the z_0 cross-sectional plane ($\langle p(r, z_0) \rangle_r \sim 0.5 p(0, z_0)$), and q is the elementary charge. The results are shown by crosses in Figure 4, and the maximum value of T_{source} is 0.6 mN for 780 W.

With the assumption that the plasma follows the conical nozzle shape (Figure 1), the additional axial force term T_{cone} from the physical nozzle of angle θ (where $r(z) = r_{end} + z \tan \theta$) from z_0 to z_{exit} (Figure 1) can be written as

$$T_{cone} = \int_{z_0}^{z_{exit}} \langle p(r, z) \rangle_r \left(\frac{dA}{dz} \right) dz, \text{ where } dA = 2\pi r_p(z) \tan \theta dz, \quad (2)$$

where the plasma radius $r_p(z)$ corresponds to the cavity radius (Figure 1). T_{cone} is calculated assuming the same variation of axial density for all rf powers as that measured for 530 W effective rf power on Figure 2 and the same variation of radial density as that measured for $z_0 = 10.5$ cm yielding an electron pressure fit in the form $p(r, z) = (1 - (\frac{r}{r_p(z)})^a)^b$ with $a = 1.5$ and $b = 0.8$. The results are shown by open triangles in Figure 4 and the maximum value of T_{cone} is about 0.4 mN for 780 W (about $0.6 \times T_{source}$). Under these assumptions, the sum of both electron pressure contributions amount to 1 mN at 780 W, which is about 20% of the measured total axial force, i.e., 40% of the measured ($T_{total} - T_{B_{field}}$) value of 2.5 mN (Figure 3).

The axial force $T_{B_{field}}$ induced by the magnetic nozzle results from an electron diamagnetic drift in a non-uniform radial density profile and can be calculated by a two-dimensional fluid model.¹⁰ Here, we use a simpler quasi one-dimensional model of the magnetic nozzle^{6,13} based on the paraxial approximation $B_z(r, z) = B_z(0, z)$ and $A(z)B_z(z) = Const. = A(z_{exit})B_z(z_{exit})$, where $A(z) = \pi r_p(z)^2$ (the plasma flow is attached to the magnetic field lines and $r_p(z)$ is the expanding plasma radius shown in Figure 1). The axial force $T_{B_{field}}$ from the magnetic nozzle is then formulated as a “physical” nozzle (as in Eq. (2)) and written as

$$T_{B_{field}} = \int_{z_{exit}}^{z_{detachment}} \langle p(r, z) \rangle_r B_z(z_{exit}) A(z_{exit}) \frac{-1}{B_z^2} \left(\frac{dB_z}{dz} \right) dz, \quad (3)$$

where $z_{detachment}$ would be the axial position of plasma detachment from the nozzle. For this calculation, $z_{detachment} = 70$ cm is used, which corresponds to an “effective” plasma radius $r_p(z)$ of 50 cm, i.e., a few cm greater than the *Irukandji* vacuum vessel inner radius. z_{exit} represents both the start of the magnetic field divergence and the end of the cavity (Figure 1). The axial profiles of density and magnetic field shown in Figure 2 allow the calculation

of $T_{B_{field}}$. The results are shown by open squares in Figure 4 and the maximum value of $T_{B_{field}}$ is 2 mN at 780 W, which is about 40% of the measured T_{total} . The calculated $T_{B_{field}}$ agrees within 20% of the directly measured maximum $T_{B_{field}}$ value of about 2.5 mN (Figure 3), giving confidence in the plasma parameters measurements.

In summary, the measured axial force imparted from a conical magneto-plasma thruster shows contributions from both the electron pressure (a force on the wall of the source) and the magnetic field pressure (a force in the region where the magnetic field diverges). Using a simplified 1D model, which approximates the force on the back and side walls of the cavity and a force on the diverging magnetic field, about 60% of the measured thrust can be accounted for. This model does not include other possible effects such as ion inertia and shear force at the radial wall.

¹M. A. Lieberman and A. J. Lichtenberg, *Principles of Plasma Discharges and Materials Processing* (Wiley-Interscience, New York, 1994).

²A. V. Arefiev and B. N. Briezman, *Phys. Plasmas* **12**, 043504 (2005).

³A. Fruchtman, *IEEE Trans. Plasma Sci.* **39**, 530 (2011).

⁴E. Ahedo and M. Merino, *Phys. Plasmas* **17**, 073501 (2010).

⁵E. Ahedo, *Phys. Plasmas* **18**, 033510 (2011).

⁶A. Fruchtman, *Phys. Rev. Lett.* **96**, 065002 (2006).

⁷K. Takahashi, T. Lafleur, C. Charles, P. Alexander, R. W. Boswell, M. Perren, R. Laine, S. Pottinger, V. Lappas, T. Harle *et al.*, *Appl. Phys. Lett.* **98**, 141503 (2011).

⁸T. Lafleur, K. Takahashi, C. Charles, and R. Boswell, *Phys. Plasmas* **18**, 080701 (2011).

⁹S. Pottinger, V. Lappas, C. Charles, and R. Boswell, *J. Phys. D* **44**, 235201 (2011).

¹⁰K. Takahashi, T. Lafleur, C. Charles, P. Alexander, and R. W. Boswell, *Phys. Rev. Lett.* **107**, 235001 (2011).

¹¹C. Charles, W. Cox, R. W. Boswell, R. Laine, and M. Perren, *Plasma Sources Sci. Technol.* **19**, 045003 (2010).

¹²M. West, C. Charles, and R. W. Boswell, *J. Propul. Power* **24**, 134 (2008).

¹³A. Fruchtman, K. Takahashi, C. Charles, and R. W. Boswell, “A magnetic nozzle calculation of the force on a plasma,” *Phys. Plasmas* (in press).